Measurement Tensors in Diffusion MRI: Generalizing the Concept of Diffusion Encoding

Carl-Fredrik Westin[1,2], Filip Szczepankiewicz[3], Ofer Pasternak[1], Evren Özarslan[1], Daniel Topgaard[4], Hans Knutsson[2], and Markus Nilsson[3]

[1] Brigham and Women's Hospital and Harvard Medical School, Boston, MA, USA
[2] Department of Biomedical Engineering, Linköping University, Linköping, Sweden
[3] Lund University Bioimaging Center, Lund University, Lund, Sweden
[4] Center for Chemistry and Chemical Engineering, Lund University, Lund, Sweden

Abstract. In traditional diffusion MRI, short pulsed field gradients (PFG) are used for the diffusion encoding. The standard Stejskal-Tanner sequence uses one single pair of such gradients, known as single-PFG (sPFG). In this work we describe how trajectories in q-space can be used for diffusion encoding. We discuss how such encoding enables the extension of the well-known scalar b-value to a tensor-valued entity we call the diffusion measurement tensor. The new measurements contain information about higher order diffusion propagator covariances not present in sPFG. As an example analysis, we use this new information to estimate a Gaussian distribution over diffusion tensors in each voxel, described by its mean (a diffusion tensor) and its covariance (a 4th order tensor).

1 Introduction

In diffusion MRI (dMRI), each millimeter-size voxel of the image contains encoded information on the micrometer-scale translational displacements of the water [1]. The vast majority of applications today focus on the simplest form of the original MRI diffusion experiment, implemented by the Stejskal-Tanner pulse sequence [2]. This sequence is based on a pair of short pulsed diffusion encoding gradients, which we will refer to as the single pulsed field gradient (sPFG) experiment. sPFG typically is used in diffusion tensor imaging (DTI), enabling popular measures such as the mean diffusion (apparent diffusion coefficient, ADC) and diffusion anisotropy (Fractional Anisotropy, FA). Although current popular diffusion measures are very sensitive to changes in the cellular architecture, they are not very specific regarding the type of change.

We are at the cusp of a completely new generation of diffusion MRI technologies, such as oscillating gradients [3], double pulsed-field gradient (dPFG) sequences [4–6], and more general waveform sequences [7]. These methods are transforming what is possible to measure, and have the potential to vastly improve tissue characterization using diffusion MRI. Our work adds to this new generation of non-conventional pulse sequences. Our method can probe features of micron-scale transport processes (and thus microstructure) that are invisible with sPFG. Fig. 1 shows three example structures (voxel distributions) that

P. Golland et al. (Eds.): MICCAI 2014, Part III, LNCS 8675, pp. 209–216, 2014.

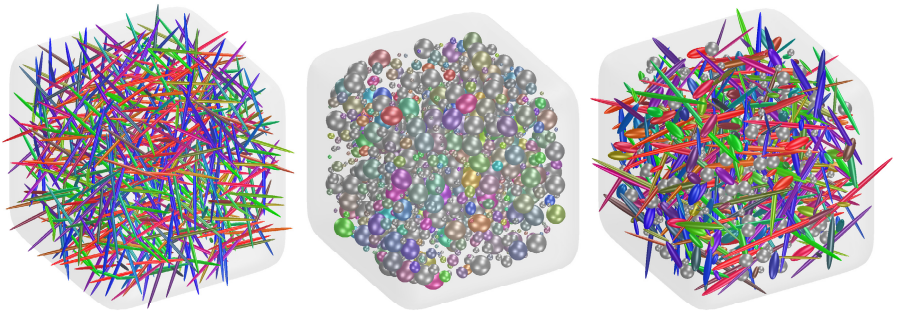

Fig. 1. Examples of globally isotropic distributions of structures within a voxel. These different structures are indistinguishable with traditional sPFG diffusion MRI.

would be indistinguishable using DTI. The aim of our work is the development of methods that can clearly distinguish these types of very different tissue architectures in clinical dMRI. In this paper, we present a new diffusion measurement framework and an example framework for analysis of the data we acquire. Together, these contributions enable us to quantify and distinguish distributions such as those in Fig. 1.

2 Theory

In conventional pulsed field gradient diffusion MRI, the diffusion encoding is achieved by applying a pair of short gradient pulses separated by a diffusion time. Such a measurement probes along a single axis in q-space. Here we will explore more general scenarios with time-varying gradients that probe trajectories in q-space. The geometry of the diffusion encoding can in the Gaussian approximation regime be described by a diffusion "measurement tensor," or "encoding tensor," which extends the traditional b-value to a tensor-valued entity. Here we define this measurement tensor by

$$\mathbf{B} = \int_0^\tau \mathbf{q}(t)\mathbf{q}^{\mathrm{T}}(t)\, dt\ , \quad \text{where} \quad \mathbf{q}(t) = \gamma \int_0^t \mathbf{g}(t')dt' \tag{1}$$

where $\mathbf{g}(t)$ is the time-dependent gradient, τ is the echo time, and γ is the gyromagnetic ratio. In this general case when the q-vector is built up by a time-dependent gradient to traverse an arbitrary path in q-space, the rank of the diffusion encoding tensor depends on the path, and is 1 in the case of sPFG, 2 for double-PFG, and 3 in the isotropic encoding case such as the triple-PFG [8] or q-MAS [9]. The conventional b-value is given by $b = \mathrm{Tr}(\mathbf{B})$, the trace of $\mathbf{B}$.

For example, a planar diffusion encoding tensor, i.e. an encoding that is rotationally symmetric in the plane (Fig. 2, left), can be achieved by a set of time

varying gradients (middle) that produce a planar q-space trajectory (right). Ideal planar encoding could be produced by a circular path in q-space. However, q-space encoding inevitably starts at the origin of q-space, so the path in Fig. 2 (right) is one way to obtain the planar encoding in practice. Constant angular b-value encoding can be ensured by varying the speed of the traversal in q-space, by using slower speed at low q-values, since the b-value is a function of both time and q-value. At a low q, a long diffusion time can build up the same encoding power (b-value), as a higher q-value with a shorter diffusion time.

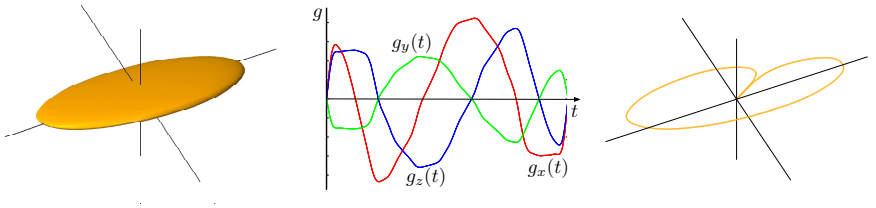

a) measurement tensor b) x-,y-,z- gradients c) q-space trajectory

Fig. 2. An example of time varying gradients (a) that produce a q-space trajectory (b) and a planar measurement tensor in b-value encoding space (c)

To generate measurement tensors $\mathbf{B}$ with general shapes one can start with q-space trajectory $\mathbf{q}_0(t)$ that produces a diffusion measurement tensor $\mathbf{B}_0 = \int_0^\tau \mathbf{q}_0(t)\mathbf{q}_0(t)^{\mathrm{T}}\, dt$ and scale the trajectory with an affine transform $\mathbf{M}$ yielding the new curve $\mathbf{q}(t) = \mathbf{M}\mathbf{q}_0(t)$. This results in a new diffusion measurement tensor $\mathbf{B}$,

$$\mathbf{B} = \int_0^\tau \mathbf{M}\mathbf{q}_0(t)\ \left(\mathbf{M}\mathbf{q}_0(t)\right)^{\mathrm{T}}\ dt \tag{2}$$

$$= \mathbf{M}\ \left(\int_0^\tau \mathbf{q}_0(t)\mathbf{q}_0(t)^{\mathrm{T}}\ dt\right)\ \mathbf{M}^{\mathrm{T}} = \mathbf{M}\ \mathbf{B}_0\ \mathbf{M}^{\mathrm{T}} \tag{3}$$

The special case of transforming a normalized isotropic curve, $\mathbf{B_0} = \mathbf{I}$, produces the simple relation $\mathbf{B} = \mathbf{M}\mathbf{M}^T$ between the affine transform and the resulting measurement tensor.

We denote dMRI with encoding performed using arbitrary trajectories of $\mathbf{q}(t)$ as q-space trajectory imaging (QTI). The measurement tensors allowed by QTI enable the separation of orientation dispersion and underlying macroscopical dispersion [10–12]. Below we propose an example analysis of QTI data where we estimate a distribution over diffusion tensors at each voxel.

3 Methods

We implemented q-space trajectory imaging (QTI) on a clinical MRI scanner (Philips Achieva 3T). Imaging parameters were: TE = 160 ms, $\mathrm{Tr}(\mathbf{B}) = b = 0$,

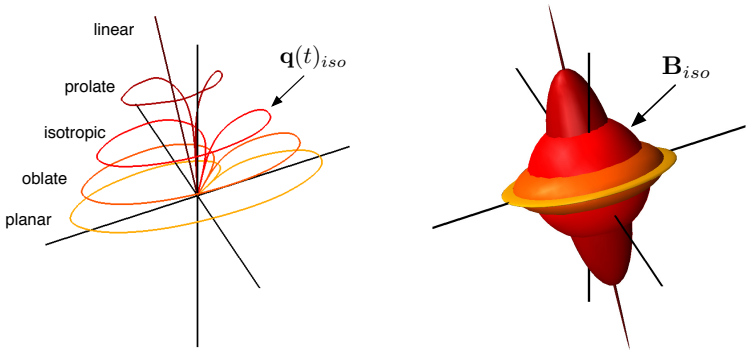

Fig. 3. Plot of five different q-space trajectories, with x-y-z axes (left). By varying the trajectory of q, diffusion encoding tensors of varying shapes can be produced. The color coding links the q-space trajectories (left) with the corresponding measurement tensors (right). The curve $\mathbf{q}(t)_{iso}$ produces a spherical b-value encoding.

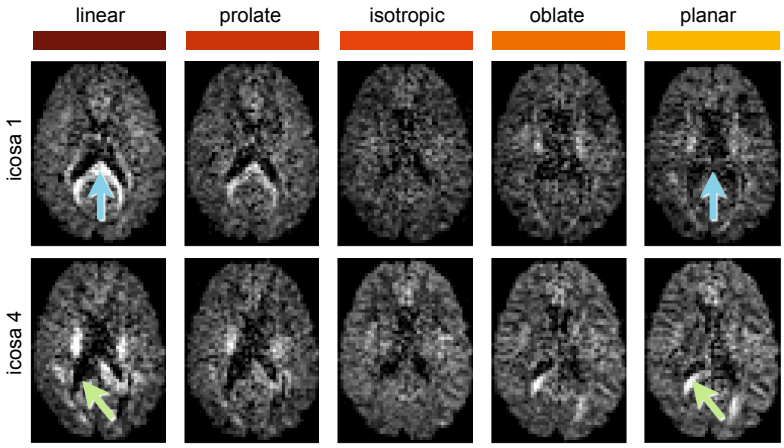

Fig. 4. MR signal from the five different types of trajectories in Fig 3, applied in two different directions in q-space. The five types of trajectories produce measurement **B**-tensors with (from left to right) linear, prolate, isotropic, oblate, and planar shapes. Note that the linear and the planar measurement are orthogonal/dual, and thus, where the linear measurement is bright the planar is dark; see blue and green arrows.

250, 500, 1000 and 2000 s/mm^2, voxel size = $3 \times 3 \times 3$ mm^3. The time varying gradients were designed to produce q-space trajectories generating linear, prolate, isotropic, oblate, and planar diffusion measurement tensors, which all were cylindrically symmetric, with the symmetry axis rotated into directions specified by the icosahedron, dodecahedron, and the truncated icosahedron. Despite the rather long TE due to our prototype implementation, the resulting diffusion encoded images were of a high image quality (Fig. 4).

3.1 Example Analysis: Estimating a Distribution over Diffusion Tensors

We propose an example analysis to demonstrate that we can measure additional microstructure information using QTI. Consider a system composed by a collection of environments, where in each environment the diffusion is Gaussian and described by the diffusion tensor $\mathbf{D}$ (as in Fig. 1). We propose to compactly model these microenvironments within a voxel with a Gaussian distribution over tensors. The tensor $\mathbf{D}$ is then a stochastic variable with expectation $\overline{\mathbf{D}} = \langle \mathbf{D} \rangle$. The covariance of $\mathbf{D}$ is given by a 4th-order tensor Σ of size $3 \times 3 \times 3 \times 3$ [13]. The description is simplified by using Voigt notation, which allows the diffusion tensor, which is normally expressed as a 3×3 matrix,

$$\mathbf{D} = \begin{pmatrix} D_{xx} & D_{xy} & D_{xz} \\ D_{yx} & D_{yy} & D_{yz} \\ D_{zx} & D_{zy} & D_{zz} \end{pmatrix} \tag{4}$$

to be represented as a 1×6 vector

$$\mathbf{d} = \begin{pmatrix} D_{xx} & D_{yy} & D_{zz} & \sqrt{2}D_{xy} & \sqrt{2}D_{xz} & \sqrt{2}D_{yz} \end{pmatrix}^{\mathrm{T}} \tag{5}$$

allowing the fourth order 4th-order tensor Σ to be represented by a 6×6 variance-covariance matrix ($\mathbb{S}$), defined using the ordinary definition of the covariance matrix $\mathbb{S} = \langle \mathbf{d}\mathbf{d}^{\mathrm{T}} \rangle - \langle \mathbf{d} \rangle \langle \mathbf{d} \rangle^{\mathrm{T}}$, and in full given by

$$\mathbb{S} = \begin{pmatrix} \Sigma_{xxxx} & \Sigma_{xxyy} & \Sigma_{xxzz} & \sqrt{2}\Sigma_{xxxy} & \sqrt{2}\Sigma_{xxxz} & \sqrt{2}\Sigma_{xxyz} \\ \Sigma_{yyxx} & \Sigma_{yyyy} & \Sigma_{yyzz} & \sqrt{2}\Sigma_{yyxy} & \sqrt{2}\Sigma_{yyxz} & \sqrt{2}\Sigma_{yyyz} \\ \Sigma_{zzxx} & \Sigma_{zzyy} & \Sigma_{zzzz} & \sqrt{2}\Sigma_{zzxy} & \sqrt{2}\Sigma_{zzxz} & \sqrt{2}\Sigma_{zzyz} \\ \sqrt{2}\Sigma_{xyxx} & \sqrt{2}\Sigma_{xyyy} & \sqrt{2}\Sigma_{xyzz} & 2\Sigma_{xyxy} & 2\Sigma_{xyxz} & 2\Sigma_{xyyz} \\ \sqrt{2}\Sigma_{xzxx} & \sqrt{2}\Sigma_{xzyy} & \sqrt{2}\Sigma_{xzzz} & 2\Sigma_{xzxy} & 2\Sigma_{xzxz} & 2\Sigma_{xzyz} \\ \sqrt{2}\Sigma_{yzxx} & \sqrt{2}\Sigma_{yzyy} & \sqrt{2}\Sigma_{yzzz} & 2\Sigma_{yzxy} & 2\Sigma_{yzxz} & 2\Sigma_{yzyz} \end{pmatrix} \tag{6}$$

To estimate $\mathbb{S}$, consider the diffusion encoded MR-signal E from a system composed of multiple environments, each having Gaussian diffusion,

$$E(\mathbf{B}) = \left\langle \exp\left(- < \mathbf{B}, \mathbf{D} >\right) \right\rangle = \left\langle \exp\left(-\mathbf{b}^{\mathrm{T}}\mathbf{d}\right) \right\rangle \tag{7}$$

where $< \cdot \, , \, \cdot >$ is the inner product, which with Voigt notation is simplified to a vector inner product $< \mathbf{B}, \mathbf{D} >= \mathbf{b}^{\mathrm{T}}\mathbf{d}$ and $\left\langle \right\rangle$ represent integration over the distribution in the voxel. Expanding the logarithm of E around $\mathbf{B} = 0$ (derivation omitted), reveals a key relationship

$$\log E(\mathbf{b}) \approx -\mathbf{b}^{\mathrm{T}}\overline{\mathbf{d}} + \frac{1}{2}\mathbf{b}^{\mathrm{T}}\mathbb{S}\mathbf{b} \tag{8}$$

where $\overline{\mathbf{d}}$ is the mean value of $\mathbf{d}$. The equation is superficially similar to the model used in Diffusional Kurtosis Imaging (DKI), however, the fourth order kurtosis

tensor employed in sPFG DKI only has 15 unique elements in contrast to the 21 elements required to fully specify $\mathbb{S}$. QTI enables the probing of these 6 extra dimensions (21-15), not visible with sPFG. To estimate the covariance $\mathbb{S}$ (6x6 representation of the 4th-order tensor Σ) from a set of dMRI measurements, first note that

$$\mathbf{b}^{\mathrm{T}}\mathbb{S}\mathbf{b} =< \mathbf{b}\mathbf{b}^{\mathrm{T}}, \mathbb{S} >=< \mathbb{B}, \mathbb{S} >= \mathbb{b}^{\mathrm{T}}\mathbb{s} \tag{9}$$

where $\mathbb{b}$ and $\mathbb{s}$ are the Voigt representation of $\mathbb{B} = \mathbf{b}\mathbf{b}^{\mathrm{T}}$ and $\mathbb{S}$, as 21×1 vectors. Since Eq. 8 is a linear model, we may estimate $\overline{\mathbf{d}}$ and $\mathbb{s}$ using pseudoinversion to solve the following equation system

$$\begin{pmatrix} \log E_1 \\ \vdots \\ \log E_m \end{pmatrix} = \begin{pmatrix} 1 & -\mathbf{b}_1^{\mathrm{T}} & \frac{1}{2}\mathbb{b}_1^{\mathrm{T}} \\ \vdots & \vdots & \vdots \\ 1 & -\mathbf{b}_m^{\mathrm{T}} & \frac{1}{2}\mathbb{b}_m^{\mathrm{T}} \end{pmatrix} \begin{pmatrix} E_0 & \overline{\mathbf{d}} & \mathbb{s} \end{pmatrix}^{\mathrm{T}} \tag{10}$$

In total, the model has 1+6+21 free parameters. $(E_0, \overline{\mathbf{d}}, \mathbb{s})$, The 21 parameters of the 4th-order tensor are difficult to interpret individually. The isotropic 4th-order tensor has, however, two components [14]

$$\mathbb{S}_{iso} = s_1\, \mathbb{E}_1 + s_2\, \mathbb{E}_2 \tag{11}$$

which in the field of mechanics are interpreted as bulk and shear modulus of the 4th-order stress tensor. The bases are given by

$$\mathbb{E}_1 = \frac{1}{3}\mathbf{e}\mathbf{e}^{\mathrm{T}} \quad \text{and} \quad \mathbb{E}_2 = \frac{3}{\sqrt{45}}(\mathbb{I} - \mathbb{E}_1) \tag{12}$$

where $\mathbb{I}$ is the 6×6 identity matrix. Note that $\mathbb{E}_1$ and $\mathbb{E}_2$ are orthogonal and normalized, i.e. $< \mathbb{E}_i, \mathbb{E}_j >= \delta_{ij}$. Expressed in full, these matrices assume simple structures according to

$$\mathbb{E}_1 = \frac{1}{3}\begin{pmatrix} 1 & 1 & 1 & 0 & 0 & 0 \\ 1 & 1 & 1 & 0 & 0 & 0 \\ 1 & 1 & 1 & 0 & 0 & 0 \\ 0 & 0 & 0 & 0 & 0 & 0 \\ 0 & 0 & 0 & 0 & 0 & 0 \\ 0 & 0 & 0 & 0 & 0 & 0 \end{pmatrix} \quad \mathbb{E}_2 = \frac{1}{\sqrt{45}}\begin{pmatrix} 2 & -1 & -1 & 0 & 0 & 0 \\ -1 & 2 & -1 & 0 & 0 & 0 \\ -1 & -1 & 2 & 0 & 0 & 0 \\ 0 & 0 & 0 & 3 & 0 & 0 \\ 0 & 0 & 0 & 0 & 3 & 0 \\ 0 & 0 & 0 & 0 & 0 & 3 \end{pmatrix} \tag{13}$$

Similarly to estimating the mean diffusivity MD by projecting the diffusion tensor on its isotropic basis element, $\mathbf{E} = \mathbf{I}/3$ (with $\mathbf{I}$ being the identity matrix), MD $=< \mathbf{D}, \mathbf{E} >$, we can project the estimated 4th-order covariance matrix onto its two isotropic basis elements $\mathbb{E}_1$ and $\mathbb{E}_2$ and obtain the parameters s_1 and s_2. These parameters can be interpreted as the bulk variation of diffusion tensors (i.e. variation in size) and the shear of them (i.e. variation between directions). Hence, s_2 contains information about microscopic anisotropy, and would give a high value for a system containing anisotropic microscopic compartments (Fig. 1, left), and a low value for isotropic compartments (Fig. 1, middle). On the other hand, s_1 reflects variation of mean diffusivities and would yield a low value if all microscopic compartments are similar in this respect (Fig. 1, left), but a high value if they are not (Fig. 1, middle).

s_1 (QTI) s_2 (QTI) FA (DTI)

Fig. 5. Bulk and shear modulus, s_1, s_2 estimated from fourth order QTI model, and FA from the DTI model

4 Results

Figure 5 shows the result of estimating the bulk and shear variation (s_1 and s_2) from QTI. The map of s_1 shows high values in regions where we expect both tissue and cerebrospinal fluid in the voxels, which leads to a high variability in mean diffusivities. By contrast, the map of s_2 is high and uniform in the white matter where variability in diffusivities is driven by the combination of high anisotropy and random orientations of the underlying microscopic environments. Since the analysis was performed on the isotropic components of the 4th order tensor, we know that all voxels have high orientation dispersion and thus s_1 reflects only underlying anisotropy. In contrast to FA from DTI, s_1 is high in regions of crossing fibers with a high orientation dispersion.

5 Discussion and Conclusions

QTI enables diffusion encoding with a general measurement tensor $\mathbf{B}$. Although the "b-matrix" concept is well established, and can be found in standard text books on diffusion NMR and MRI, the characterization of the b-matrix using double-PFG, and more general gradient wave form diffusion MRI is novel and different. In current literature, the concept of b-matrix normally refers to the standard rank-one measurement (in our terminology) with added imaging gradient and other correction terms. Extending the traditional rank-1 diffusion measurement, to rank-2 and full rank-3 measurements, allows for measuring information that was previously not attainable.

Our work shows that it is possible to perform diffusion encoding imaging of the human brain with arbitrary q-space trajectories while maintaining good SNR, and generalizes the concept of b-values enabling new types of measurements not available with sPFG.

Acknowledgments. The authors acknowledge the NIH grants R01MH074794, R01MH092862, P41-RR013218, P41EB015902, and the Swedish Research Council (VR) grants 2012-3682, 2011-5176, 2011-4334, and Swedish Foundation for Strategic Research grant AM13-0090.

References

1. Callaghan, P.T.: Translational dynamics and magnetic resonance: principles of pulsed gradient spin echo NMR. Oxford University Press (2011)
2. Stejskal, E.O., Tanner, J.E.: Spin diffusion measurements: Spin echoes in the presence of a time-dependent field gradient. J. Chem. Phys. 42(1), 288–292 (1965)
3. Does, M.D., Parsons, E.C., Gore, J.C.: Oscillating gradient measurements of water diffusion in normal and globally ischemic rat brain. MRM 49(2), 206–215 (2003)
4. Cory, D.G., Garriway, A.N., Miller, J.B.: Applications of spin transport as a probe of local geometry. Polym. Prepr. 31, 149–150 (1990)
5. Mitra, P.P.: Multiple wave-vector extensions of the NMR pulsed-field-gradient spin-echo diffusion measurement. Physical Review B 51(21), 15074 (1995)
6. Callaghan, P., Komlosh, M.: Locally anisotropic motion in a macroscopically isotropic system: displacement correlations measured using double pulsed gradient spin-echo NMR. Magnetic Resonance in Chemistry 40(13), S15–S19 (2002)
7. Drobnjak, I., Alexander, D.C.: Optimising time-varying gradient orientation for microstructure sensitivity in diffusion-weighted MR. JRM 212(2), 344–354 (2011)
8. Valette, J., Giraudeau, C., Marchadour, C., Djemai, B., Geffroy, F., Ghaly, M.A., Le Bihan, D., Hantraye, P., Lebon, V., Lethimonnier, F.: A new sequence for single-shot diffusion-weighted nmr spectroscopy by the trace of the diffusion tensor. MRM 68(6), 1705–1712 (2012)
9. Eriksson, S., Lasic, S., Topgaard, D.: Isotropic diffusion weighting in PGSE NMR by magic-angle spinning of the q-vector. JMR 226, 13–18 (2012)
10. Lasic, S., Szczepankiewicz, F., Eriksson, S., Nilsson, M., Topgaard, D.: Microanisotropy imaging: quantification of microscopic diffusion anisotropy and orientational order parameter by diffusion MRI with magic-angle spinning of the q-vector. Frontiers in Physics 2(11) (2014)
11. Jensen, J.H., Hui, E.S., Helpern, J.A.: Double-pulsed diffusional kurtosis imaging. NMR in Biomed. (2014)
12. Jespersen, S.S.N., Lundell, H., Snderby, C.K., Dyrby, T.B.: Orientationally invariant metrics of apparent compartment eccentricity from double pulsed field gradient diffusion experiments. NMR in Biomed. 26(12), 1647–1662 (2013)
13. Basser, P.J., Pajevic, S.: Spectral decomposition of a 4th-order covariance tensor: Applications to diffusion tensor MRI. Signal Processing 87(2), 220–236 (2007)
14. Moakher, M.: Fourth-order cartesian tensors: old and new facts, notions and applications. The Quart. Jour. of Mechanics and Applied Math. 61(2), 181–203 (2008)